Etuk Sunday Edet[1], Robert Ubong Williams[2], Agbasi, Okechukwu Ebuka[3], Inyang Namdie Joseph[1]*

[1]Department of Physics, University of Uyo, Uyo, Akwa Ibom State, Nigeria; [2]Department of Physics, Akwa Ibom State University, Ikot Akpaden, Mkpat Enin, Akwa Ibom State, Nigeria; [3]Okna Geophysical Services, Eket, Nigeria

Scientific Paper
ISSN 0351-9465, E-ISSN 2466-2585
https://doi.org/10.62638/ZasMat1051

Zastita Materijala 65 (4)
660 – 667 (2024)

Influence Of Rice Husk Ash Inclusion On Electrical Characteristics Of Dry Cement Mortar

ABSTRACT

Rice husk is usually generated as waste in large quantities but yet to be optimally utilized. Due to the pollution effects associated with poor approach prevalently adopted for its disposal, volarizing it into economical and sustainable material for building construction is a necessary option to provide solution for future generation. In this research, separate dry mortars were prepared using cement grades 32.5R and 42.5N and the influence of rice husk ash (RHA) inclusion on their electrical characteristics was investigated. The materials used were batched by volume and the RHA was utilized as a partial substitute for cement at 10 % level. All the samples were cured for 21 days and then allowed to dry completely prior to the tests implementation. The results showed decrease in electrical resistance with temperature (ranging from 20°C to 50°C) due to incorporation of the RHA. Though samples with the RHA content possessed ability to act as smart mortars for temperature monitoring/sensing, utilization of cement grade 42.5N ensured a better performance. By utilizing rice husks in such undertakings, their associated disposal problems could be tackled and construction of inexpensive but sustainable building with large temperature sensing capability could be enhanced.

Keywords: *Building; Electrical resistance; Temperature sensing; Thermal sensitivity index; Waste*

1. INTRODUCTION

Mortar is homogeneous mixture of cementitious material, fine aggregate (sand), and specific amount of water. In building construction, cement mortar is used for plastering over bricks or other forms of masonry. The knowledge acquired from the study of electrical properties of cement-based composites has helped to understand that cement mortar can perform other interesting functions. For instance, Ahmed and Kamal [1] observed that conductive cement mortar has amazing infrastructural applications including building surface heating, pavement de-icing, electromagnetic defence, cathodic protection, and enhancing foundations and buried ground grid systems. Also, Honorio et al [2] found that electrical resistivity and conductivity provide useful information on the durability of cement-based materials and can be used for monitoring and inspection of concrete structures. Bazari and Chini [3] noticed that it is possible to fully observe the setting time and compressive strength of mortar and concrete by electrical resistance method than in the case of employing common physical tests.

In recent times, researchers have investigated different replacements for conventional materials as well as additives to conventional mortars in order to improve the properties of the cementitious composites. Such filler materials include carbon fiber [4 – 6], graphene [6, 7], carbon black [9 – 12], and carbon nanofiber [13]. The use of carbon nanotube yields reinforced composites that have excellent function properties, such as mechanical properties [14], high-temperature properties [15 – 17], and electrical properties [18 – 21]. Among other factors, the behavior of the composites is influenced by the kind of filler material used. For example, Yoo et al [22] observed that multi-walled carbon nanotubes have

* Corresponding author: Okechukwu, Ebuka Agbasi
E-mail: agbasi.okechukwu@gmail.com
Paper received: 27.03.2024.
Paper accepted: 3.05.2024.
Papir is available on the website: www.idk.org.rs/journal

a better enhancement effect on the electrical conductivity of cement paste than graphite nanofibers and graphene. But absolute reliance on these industrial waste materials could hinder sustainable development as some of them are scarce and uneconomical. Therefore, there is need to urgently consider preparation of conductive filler materials from waste that is sustainable.

The aim of this research is to examine the electrical characteristics of dry cement mortars that contain rice husk ash (RHA) as a partial replacement material for cement. In this study, two different grades of cement will be considered and the possible application(s) of the mortars will be predicted. A similar study reported in the literature involved the use of coconut husk ash and one type of cement grade [23]. The choice of rice husk for synthesis of the ash is due to its sustainability as it is continuously abundant and cheaply available in large quantity as an agro-waste. Globally, the annual output of rice husk is at least 80 million tons and over 97 % of the husk is generated in developing countries [24, 25]. Though attempts have been made to use rice husk to prepare ash for enhancement of compressive strength of concrete [26 - 28] and amendment of soil behavior [29, 30], it still remains under-utilized. With persistence of inefficient solid waste management systems in developing countries [31, 32], rice husks are prevalently disposed of by indiscriminate dumping. This situation is detrimental to the environment and needs to be addressed.

2. EXPERIMENTAL PERSPECTIVE

2.1. Materials and their description

Two different grades of Portland limestone cement (CEM II/BL 32.5 R and CEM II/BL 42.5N, both of which are manufactured by Dangote Cement PLC, Obajana Plant), sand (fine aggregate), water (from bore-hole), and rice husks were the major materials utilized in this research. The cement and sand were obtained from a building construction site. The rice husks were gathered as waste from a local rice mill. These materials were collected in large quantities within Ini Local Government Area, Akwa Ibom State, Nigeria.

2.2. Materials processing and analysis

The husks were soaked in water in order to remove dirt and other forms of impurities from them. They were removed from the water after 2 hours, sun-dried completely, and then incinerated in an open air. The ash obtained was screened using standard US sieve No 200. The fraction of it that passed through the sieve was kept in an air-tight container and labelled RHA. This was necessary to avoid pre-hydration during storage. With the aid of an X-ray diffractometer (Model XRD 3000P, Seifert, Germany), the scanning electron microscopic (SEM) image of the RHA was obtained to reveal its surface structure. Also, the sand was dried in the air before it was subjected to gradation test by sieving technique [33]. Loose density and angle of repose of the RHA, sand, and cement were determined as detailed elsewhere [34]. The RHA and cement were analyzed for chemical composition by adopting the method of Yahaya [35].

2.3. Samples preparation

The mix design used in this research is summarized in Table 1. All batching processes were by volume method. In each case, the cement was replaced with 10 % of the RHA. This proportion of the RHA was chosen based on the fact that it is optimum for significant results [26, 27]. When the materials were thoroughly mixed with water, each mixture was cast into separate Plexiglas molds of cross-section 52 mm x 24 mm and height 14 mm. immediately after casting and compaction, two copper plates (each with a width of 15 mm and a height of 30 mm) were embedded into the mixture. These copper plates served as electrodes and they were at same distances from the ends of the samples. The electrodes spacing and embedment length were 32 mm

Table 1. Design of the materials proportioning

Cement grade	Sample code	Constituent materials	Number of samples prepared and tested	w - c ratio
32.5 R	BCM	Sand and Cement	10	0.5 (Constant)
	RCM	Sand, RHA, and Cement	10	
42.5 N	PCM	Sand and Cement	10	
	CRM	Sand, RHA, and Cement	10	

w – c: Water – cement

and 9 mm respectively. All the samples were demolded after 24 hours and they were cured in a shade by sprinkling equal volumes of water on them twice (morning and evening) daily. The curing was allowed for 21 days after which the samples were allowed to dry completely before they were tested.

2.4. Testing of the samples

Figure 1 shows the schematic diagram of the setup used in this research. The aluminium block measured 80 mm in height and 75 mm in diameter and its use was necessary since the heating element of the hotplate was larger than the sample. In order to ensure that heat flowed upwardly only through the sample, the use of the thermal insulant (of very low thermal conductivity with dimensions 60mm x 60 mm) was necessary. This thermal insulant was provided with a central and circular hole to allow for free passage of heat from the aluminium block. Separate but identical aluminium blocks, thermal insulants, and digital thermometers (Model 305 quipped with type-K probe) were used for different test schedules. Before the commencement of the test, the sample and its electrodes were thickly lagged with cotton wool.

The electrical resistances were measured by means of LCR meter (Model No. 9183, Lutron). The probes of the meter were connected to the electrodes and the control dial on the hotplate was adjusted to a level reasonable enough to ensure a steady heat flow from the heating element. The temperature of the sample was monitored and measured with the aid of the thermometer. During this process, care was taken to ensure that the thermometer probe was in firm contact with the sample's surface as illustrated in the diagram. Temperature readings were taken at 5°C intervals from 20°C. After that, the mean and corresponding standard error values of the resistance were computed for each sample.

The electrical resistivity of the sample was determined using the formula [23]

$$R = \frac{\rho L}{A} \quad (1)$$

where R = mean electrical resistance, A = area of the sample's surface in contact with the electrodes, L = distance between the electrodes.

The value of thermal sensitivity index, β was deduced from the graph of lnR against the inverse of absolute value of the temperature, T based on the relation [36, 37]

$$R = R_o exp\left[\frac{\beta}{T}\right] \quad (2)$$

where R_o = electrical resistance at infinite temperature.

In each case, the temperature coefficient of resistance, α was computed as [38]

$$\alpha = \pm\left[\frac{1}{R_1}\left(\frac{R_2 - R_1}{T_2 - T_1}\right)\right]100\% \quad (3)$$

where R_1 and R_2 represent the values of electrical resistance obtained at temperatures T_1 and T_2 respectively.

(The negative sign is considered only if R and T relate inversely).

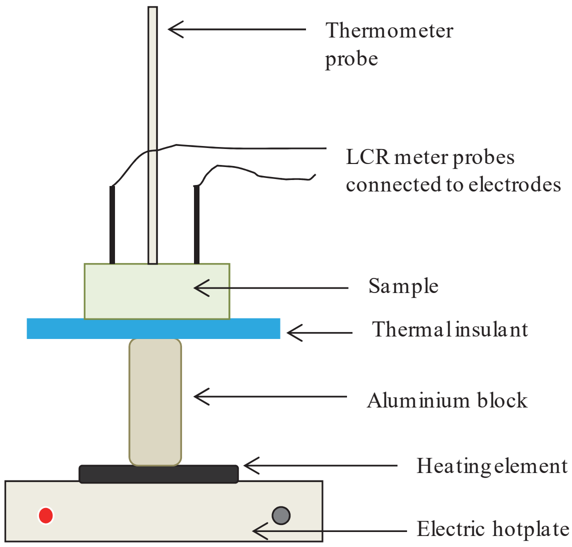

Fig. 1. Schematic features of the experimental setup

3. RESULTS AND DISCUSSION

The index properties of the constituent materials (RHA, sand, and cement) are presented in Table 2. It is clear from the results that sand is the heaviest, followed by cement, and then the RHA. Sand has the least static angle of repose value. Since repose angle of 40° is acceptable for manufacturing purposes [39], it can be adjudged that all the materials in this case are suitable for preparation of the mortars. Considering the fact that angle of repose correlates inversely with particle size of a material [40, 41], it can be inferred that particles of the sand are larger in size than those of the RHA or cement. Figure 2 depicts that the sand contains particles of assorted sizes, thereby making it to be well-graded for use.

Table 2. Particulars of the constituent materials

Parameters	RHA	Sand	Cement	
			32.5 R	42.5 N
Loose density (kgm^{-3})	370.0	1519.0	857.0	853.0
Static angle of repose (°)	39.1	34.8	39.6	39.9

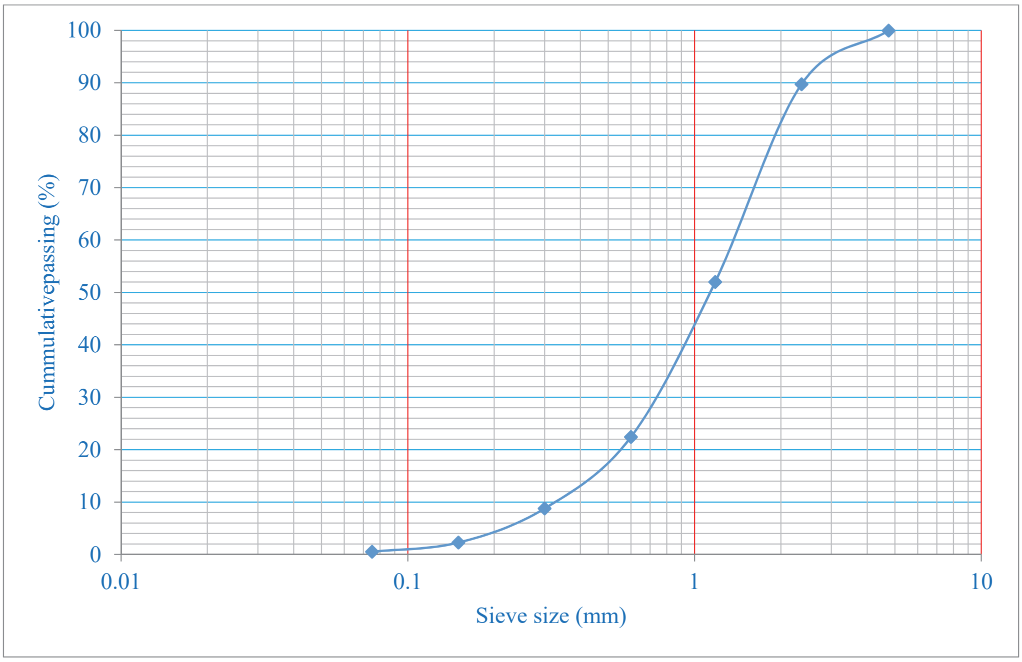

Fig. 2. Grading curve of the sand used

From the results of chemical composition analysis of the RHA and cement (Table 3), it is seen that the most abundant oxide is SiO_2 in the RHA and CaO in both grades of the cement. The loss on ignition (LOI) of cement grade 42.5N is the least while that of cement grade 32.5R is the highest. This is not out of expectation because cement grade 32.5R used in this research contains about 21 % to 30 % of limestone as stated in cement literature. Also, the value of LOI obtained for the RHA exceeds that of cement grade 42.5N, thereby indicating that it has higher content of carbon-based component than the cement. The proportions of SiO_2, Al_2O_3, and Fe_2O_3 in the RHA sum up to a value (71.69 %) which is slightly greater than 70 % required as minimum percentage for pozzolans. Thus, it can be remarked that the RHA utilized in this research is pozzolanic.

Table 3. Chemical composition of the RHA and Cement

Oxides		Proportion (%) per material		
		RHA	Cement	
Name	Formula		32.5 R	42.5 N
Silicon oxide (Silica)	SiO_2	69.88	16.32	20.82
Aluminium oxide (Alumina)	Al_2O_3	1.32	3.60	4.96
Ferric oxide	Fe_2O_3	0.48	2.83	3.20
Magnesium oxide (Magnesia)	MgO	0.59	0.90	2.12
Calcium oxide (Lime)	CaO	0.73	58.25	62.46
Loss on ignition	LOI	8.34	10.31	2.99

Figure 3 shows the monograph of the RHA. It can be clearly seen that the surface of the RHA is irregular in nature and is typical of amorphous ash. Hence, it has the potential for high reactivity.

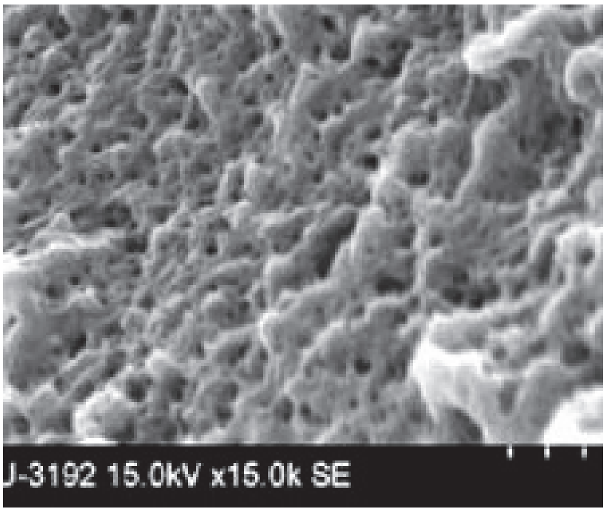

Fig. 3. SEM image of the RHA

It is noticed from the results in Table 4 that at each considered temperature, inclusion of the RHA reduces the electrical resistance of the samples with respect to a particular cement grade. Figure 4 reveals that the electrical resistance in all the cases decreases with increase in temperature of the samples. This means that the samples become more electrically-conductive at higher temperatures. The observed decay pattern of the resistance-temperature relationship typifies a negative temperature coefficient (NTC) thermistor. Robert et al [23] reasoned that such phenomenal tendency is due to activation energy associated with the electron jumping across interfaces in dry cement-based composites. As such, the observed phenomenon could be utilized for temperature monitoring. On the strength of that consideration, samples with the RHA content would show better performance. Durairaj et al [42] reported that addition of brass fiber as an electrically conductive filler to cement mortar reduced the electrical resistance and also improved self-sensing ability of the mortar at elevated temperatures.

Table 4. Electrical resistance of the samples at various temperatures

Temperature, T (°C)	Mean measured electrical resistance, R (10^6 Ω)			
	BCM	RCM	PCM	CRM
20.0	57.06	18.89	56.47	17.98
25.0	25.42	9.94	24.98	9.43
30.0	12.50	5.49	11.64	4.88
35.0	6.65	3.07	5.88	2.79
40.0	2.71	1.86	2.67	1.67
45.0	1.35	1.26	1.28	1.19
50.0	0.96	0.61	0.91	0.51

Based on the electrical resistance values obtained for the samples, CRM has a greater ability than RCM for temperature sensing. The improved self-sensing abilities of the RCM and CRM over the BCM and PCM respectively could be of some great benefits if they are applied for plastering purpose. This is because, in that case, a large sensing volume is possible and in turn, it could save cost as embedded sensors conventionally used for temperature monitoring are very expensive but yet location-specific in their performance [23].

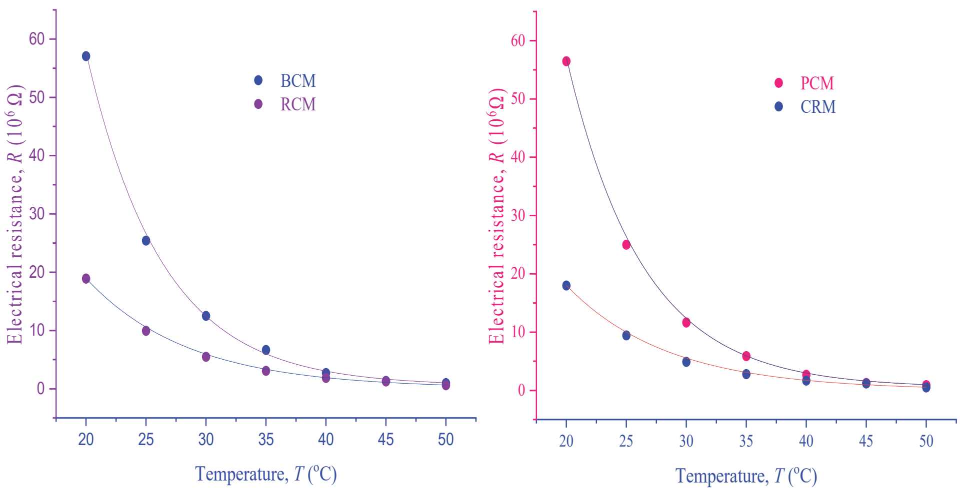

Fig. 4. Electrical resistance – temperature relationships for the samples

The plots in figure 5 agree with linearization of equation 2 above depicting how the thermal sensitivity (β-parameter) relates with inverse values of absolute temperatures of the samples. The summary of the data deduced for the samples from their resistance measurements are shown in Table 5. The electrical resistivity values support the earlier submission that the RHA enhances reduction of electrical resistance of the resulting sample in each case at a given temperature. Accordingly, 66.80 % reduction in electrical resistivity is yielded for preparing RCM over the BCM. Also, 68.06 % decrement is possible in the case of preparing CRM over PCM. This further substantiates the above-stated fact that CRM responds faster than RCM for temperature sensing though both contain the RHA. It also shows that cement grade could influence the electrical behavior of the mortar aside the known fact that it affects the 28-day compressive strength of cementitious materials.

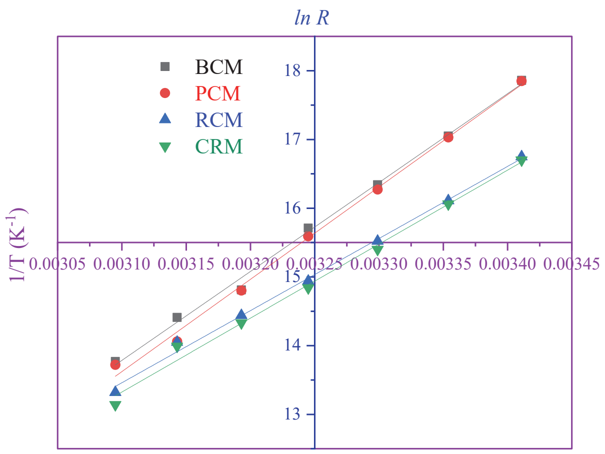

Fig. 5. Plots of In R against 1/T

Table 5. Computed values of electrical parameters of the samples

Sample code	ρ (10^5 Ωm) 20°C	at β (K)	α (% /°C)
BCM	2.41	12937	-3.277
RCM	0.80	10493	-3.226
PCM	2.38	13457	-3.280
CRM	0.76	10763	-3.239

Based on the β-values obtained in this study, it can be averred that RCM and CRM require smaller energy for electrical conduction compared to the BCM and PCM respectively being their counterparts without the RHA content. By implication, the RHA has the potential to lower energy needed by cement mortar for sensing role. The temperature coefficients of resistance obtained in this study show that the samples could be used as NTC thermistors and temperature sensors

5. CONCLUSION

The investigations carried out in this research revealed that inclusion of 10 % RHA as partial cement substitute caused a significant influence on electrical characteristics of the resulting dry cement mortars. Electrical resistivity and thermal sensitivity index values were lowered as a result of RHA introduction into each plain cement mortar. Electrical resistances of the samples exhibited exponential decay with increase in temperature, thereby indicating that the samples have negative temperature coefficient of resistance. Though samples with the RHA content could be regarded as promising smart mortars, it was observed that utilization of cement grade 42.5N yielded a better self-sensing mortar sample. Thus, if the mortars with RHA content are applied for plastering, building structures can effectively monitor/sense their own temperature without any need for attached sensors.

REFERENCES

[1] S.M.Ahmed, I.Kamal (2022) Electrical resistivity and compressive strength of cement mortar based on green magnetite nanoparticles and wastes from steel industry. Case Stud/ Const. Mat., 17, e01712, https://doi.org/10.1016/j.cscm.2022.e01712

[2] T.Honorio, H.Carasek, O.Cascudo (2020) Electrical properties of cement-based materials: Multiscale modeling and quantification of the variability. Const. Build. Mat., 245, 11846. https://doi.org/10.1016/j.conbuildmat.2020.118461. hal-02486901

[3] A.A.K.Bazari, M.Chini (2022) Laboratory Evaluation of Electrical Resistance of Concrete. J. Civ. Eng. Mat. App. 6, 99 – 111, https://doi.org/10.22034/jcema.2022.333341.1082

[4] C.Vipulanandan, A.Mohammed (2015) Smart cement modified with iron oxide nanoparticles to enhance the piezoresistive behaviour and compressive strength for oil well applications. Smart Mater. Struct. 24, 125020.

[5] M.Chen, P.Gao, F.Geng, L.Zhang, H.Liu (2017) Mechanical and smart properties of carbon fiber and graphite conductive concrete for internal damage monitoring of structure. Const. Build. Mat. 142, 320 – 327

[6] B.Han, L.Zhang, S.Sun, X.Yu, X.Dong, T.Wu, J.Ou (2015) Electrostatic self-assembled carbon nanotube/nano carbon black composite fillers reinforced cement-based materials with multifunctionality. Compos. Part A Appl. Sci. Manuf. 79, 103 – 115

[7] Q.Liu, W.Wu, J.Xiao, Y.Tian, J.Chen, A.Singh (2019) Correlation between damage evolution and resistivity reaction of concrete in-filled with graphene nanoplatelets. Constr. Build. Mater, 208, 482 – 491

[8] O.E.Ozbulut, Z.Jiang, D.K.Harris (2018) Exploring scalable fabrication of self-sensing cementitious composites with grapheme na-noplatelets, Smart Mater. Struct. 7, 115029

[9] A.Monteiro, P.Cachim, P.M.Costa (2017) Self-sensing piezoresistive cement composite loaded with carbon black particles. Cem. Concr. Compos. 81, 59 – 65

[10] Z.Jiang, O.E.Ozbulut, G.Xing (2019) Self-Sensing Characterization of GNP and carbon black filled cementitious composites. In: Proceedings of the ASME 2019 Conference on Smart Materials, Adaptive Structures and Intelligent Systems, Louisville, KY, USA, 9 – 11 September 2019.

[11] Y.Ding, G.Liu, A.Hussain, F.Pacheco-Torgal, Y.Zhang (2019) Effect of steel fiber and carbon black on the self-sensing ability of concrete cracks under bending. Constr. Build. Mater. 2017, 630 – 639.

[12] G.Yıldırım, M.H.Sarwar, A.Al-Dahawi, O.Öztürk, O.Anıl, M.Sahmaran (2018) Piezoresistive behavior of CF-and CNT-based reinforced concrete beams subjected to static flexural loading: Shear failure investigation. Constr. Build. Mater. 168, 266 – 279

[13] T.Buasiri, K.Habermehl-Cwirzen, L.Krzeminski, A.Cwirzen (2021) Role of Carbon Nanofiber on the Electrical Resistivity of Mortar under Compressive Load. Trans. Res. Recl. 2675, 33 – 37, https://doi.org/10.1177/0361198120947417

[14] F.Gao, W.Tian, Z.Wang, F.Wang (2020) Effect of diameter of multi-walled carbon nanotubes on mechanical properties and microstructure of the cement-based materials. Const. Build. Mat. 260, 120452

[15] F.Gao, W.Tian, X.Cheng (2021) Investigation of moisture migration of MWCNTs concrete after different heatingcooling process by LF-NMR. Const. Build. Mat. 288, 123146

[16] A.Sedaghatdoost, K.Behfarnia (2018) Mechanical Properties of Portland Cement Mortar Containing Multi-Walled Carbon Nanotubes at Elevated Temperatures. Constr. Build. Mater. 176, 482–489.

[17] W.L.Baloch, R.A.Khushnood, W.Khaliq (2018) Influence of Multi-Walled Carbon Nanotubes on the Residual Performance of Concrete Exposed to High Temperatures. Constr. Build. Mater. 185, 44–56.

[18] G.M.Kim, H.N.Yoon, H.K.Lee (2018) Autogenous Shrinkage and Electrical Characteristics of Cement Pastes and Mortars with Carbon. Constr. Build. Mater.177, 428 - 435

[19] A.Abdulhameed, N.Z.A.Wahab, M.N.Mohtar, M.N.Hamidon, S.Shafie, I.A.Halin (2021) Methods and applications of electrical conductivity enhancement of materials using carbon nanotubes. J. Electron. Mater., 50(6), 3207–3221.

[20] S.H.Jang, D.P.Hochstein, S.Kawashima, H.Yin (2017) Experiments and micromechanical modeling of electrical conductivity of carbon nanotube/cement composites with moisture. Cem. Concr. Compos., 77, 49–59.

[21] S.Ding, S.Dong, A.Ashour, B.Han (2019) Development of sensing concrete: principles, properties and its applications. J. Appl. Phys., 126(24), 241101.

[22] D.Y.Yoo, I.You, S.J.Lee (2018) Electrical and piezoresistive sensing capacities of cement paste with multi-walled carbon nanotubes. Eng. 18(2), 371–384.

[23] U.W.Robert, S.E.Etuk, S.A.Ekong, O.E.Agbasi, N.E.Ekpenyong, S.S.Akpan, E.A.Umana (2022) Electrical characteristics of dry cement-based composites modified with coconut husk ash nanomaterial. Adv. Mater. Sci., 22, 64–77, https://doi.org/10.2478/adms-2022-0008.

[24] T.Honorio, B.Bary, J.Sanahuja, F.Benboudjema (2017) Effective properties of n-coated composite spheres assemblage in an ageing linear viscoelastic framework. Int. J. Solids Struct.,, 124, 1–13.

[25] J.C.Nadeau (2002) Water-cement ratio gradients in mortars and corresponding effective elastic properties. Cem. Concr. Res., 32(3), 481–490.

[26] M.Amin, B.A.Abdelsalam (2019) Efficiency of rice husk ash and fly ash as reactivity materials in sustainable concrete. Sustain. Environ. Res., 29, Article 30, https://doi.org/10.1186/s42834-019-0035-2.

[27] O.Zaid, J.Ahmad, M.S.Siddique, F.Aslam (2021) Effect of Incorporation of Rice Husk Ash instead of Cement on the Performance of Steel Fibers Reinforced Concrete. Front. Mater., 8, 665625, https://doi.org/10.3389/fmats.2021.665625.

[28] B.Bheel, A.W.Abro, I.A.Shar, A.A.Dayo, S.Shaikh, Z.H.Shaikh, (2019) Use of Rice Husk Ash as Cementitious Material in Concrete. Eng. Technol. Appl. Sci. Res. 9(3), 4209–4212.

[29] M.Yin, X.Li, Q.Liu, F.Tang (2022) Rice husk ash addition to acid red soil improves the soil property and cotton seedling growth. Sci. Rep., 12, 1704, https://doi.org/10.1038/s41598-022-05199-7.

[30] P.Saranya, C.M.Sri Gayathiri, K.M.Sellamuthu (2018) Potential Use of Rice Husk Ash for Enhancing Growth of Maize (Zea mays). Int. J. Curr. Microbiol. Appl. Sci., 7(3), 899–906, https://doi.org/10.20546/ijcmas.2018.703.105.

[31] U.W.Robert, S.E.Etuk, O.E.Agbasi, S.A.Ekong, E.U.Nathaniel, A.Anonaba, L.A.Nnana (2021) Valorization of Waste carton paper, Melon seed husks and Groundnut shells to thermal insulation panels for structural applications. Polytechnica., 4(2), 97–106, https://doi.org/10.1007/s41050-021-00034-w.

[32] S.A.Ekong, D.A.Oyegoke, A.A.Edema, U.W.Robert (2022) Density and water absorption coefficient of sandcrete blocks produced with waste paper ash as partial replacement of cement. Adv. Mater. Sci., 22(4), 85–97, https://doi.org/10.2478/adms-2022-0021.

[33] ASTM C136/136M (2019) Standard Test Method for Sieve Analysis of Fine and Coarse Aggregates. ASTM International, West Conshohocken, PA.

[34] U.W.Robert, S.E.Etuk, O.E.Agbasi, U.S.Okorie, Z.T.Abdulrazzaq, A.U.Anonaba, O.T.Ojo (2021) On the hygrothermal properties of sandcrete blocks produced with sawdust as partial replacement of sand. J. Mech. Behav. Mater., 30(1), 144–155, doi.org/10.1515/jmbm-2021-0015.

[35] M.D.Yahaya (2009) Physico-chemical classification of Nigerian cement. Aust. J. Technol., 12(3), 164–174.

[36] S.E.Etuk, J.B.Emah, U.W.Robert, O.E.Agbasi, I.A.Akpabio (2021) Comparison of Electrical Resistivity of Soots formed by combustion of Kerosene, Diesel, aviation fuel and their mixtures. Brilliant Eng., 3, 6–10, https://doi.org/10.36937/ben.2021.003.002.

[37] S.S.Munifah, A.Wiendartun, A.Aminudim (2018) Design of temperature measuring instrument using NTC thermistor of Fe2TiO5 based on microcontroller AT mega 328. J. Phys.: Conf. Ser., IOP Publishing, 1–7.

[38] U.W.Robert, S.E.Etuk, O.E.Agbasi, U.A.Iboh, S.S.Ekpo (2020) Temperature-Dependent Electrical Characteristics of Disc-shaped Compacts fabricated using Calcined Eggshell Nanopowder and Dry Cassava starch. Powder Metall. Prog., 20(1), 12–20, http://dx.doi.org/10.2478/pmp-2020-0002.

[39] A.O.Adeniran, A.O.Akankpo, S.E.Etuk, U.W.Robert, O.E.Agbasi (2022) Comparative study of electrical resistance of disc-shaped compacts fabricated using calcined clams shell, Periwinkle shell and Oyster shell nanopowder. Kragujevac J. Sci., 44, 25–36, https://doi.org/10.5937/KgJSci2244025A.

[40] X.Guiling, C.Xiaoping, L.Cai, X.Pan, Z.Changsui (2016) Experimental investigation on the flowability properties of cohesive carbonaceous powders. J. Partic. Sci. Technol., 35(3), 322–329. doi.org/10.1080/02726351.2016.1154910.

[41] H.Lu, X.Guo, Y.Liu, X.Gong (2015) Effects of particle size on flow mode and flow characteristics of pulverised coal. Kona Powder Part I., 32, 143–53. doi.org/10.14356/kona.2015002.

[1] [42] R.Durairaj, T.Varatharajan, S.K.Srinivasan, B.G.A.Gurupatham, K.Roy (2022) An Experimental Study on Electrical Properties of Self-Sensing Mortar. J. Compos. Sci., 6, 1–28, https://doi.org/10.3390/jcs6070208.

IZVOD

UTICAJ INKLUZIJE PEPELA OD PIRINČANE LJUSKE NA ELEKTRIČNE KARAKTERISTIKE SUVOG CEMENTNOG MALTERA

Pirinčana ljuska se obično stvara kao otpad u velikim količinama, ali tek treba da se optimalno iskoristi. Zbog efekata zagađenja povezanih sa lošim pristupom koji se uglavnom koristi za njegovo odlaganje, pretvaranje u ekonomičan i održiv materijal za izgradnju zgrada je neophodna opcija za obezbeđivanje rešenja za buduće generacije. U ovom istraživanju odvojeni suvi malteri su pripremljeni korišćenjem cementa 32,5R i 42,5N i ispitan je uticaj pepela pirinčane ljuske (RHA) na njihove električne karakteristike. Korišćeni materijali su dozirani po zapremini i RHA je korišćen kao delimična zamena za cement na nivou od 10%. Svi uzorci su sušeni 21 dan, a zatim ostavljeni da se potpuno osuše pre sprovođenja testa. Rezultati su pokazali smanjenje električnog otpora sa temperaturom (u rasponu od 20°C do 50°C) usled ugradnje RHA. Iako su uzorci sa sadržajem RHA posedovali sposobnost da deluju kao pametni malteri za praćenje/senzivanje temperature, korišćenje cementa 42,5N je obezbedilo bolje performanse. Korišćenjem pirinčanih ljuski u takvim poduhvatima, mogli bi se rešiti njihovi povezani problemi odlaganja i poboljšati izgradnja jeftine, ali održive zgrade sa velikom sposobnošću senzora temperature.

Ključne reči: *zgrada; Električna otpornost; Senzor temperature; Indeks toplotne osetljivosti; Gubljenje*

Naučni rad

Rad primljen: 27.03.2024.

Rad prihvaćen: 3.05.2024.

The ORCID Ids of all the authors are as follows:

1. Sunday Edet Etuk: https://orcid.org/0000-0002-2573-8314

2. Ubong Williams Robert: https://orcid.org/0000-0001-9979-7176

3. Okechukwu Ebuka Agbasi: https://orcid.org/0000-0001-5649-0107

4. Namdie Joseph Inyang: https://orcid.org/0000-0002-8798-4692